Hydrology Research



Hydrology Research Vol 00 No 0, 1 doi: 10.2166/nh.2023.206

# Selecting criteria for urban basin delineation based on UAV photogrammetry: a case study in Culiacan, Mexico

Sergio Arturo Renteria-Guevara[a], Jesus Gabriel Rangel Peraza[b,*], Abel Rivera-Buelna[a], Sergio Alberto Monjardin-Armenta[c], Antonio Jesus Sanhouse-Garcia[b] and Fernando Garcia-Paez[c]

[a] Facultad de Ingenieria Civil, Universidad Autónoma de Sinaloa, Circuito Interior Oriente, Cd Universitaria, Culiacán, Sinaloa 80040, México
[b] Tecnológico Nacional de México/Instituto Tecnológico de Culiacán, Juan de Dios Bátiz 310, Col. Guadalupe, Culiacán, Sinaloa 80220, México
[c] Facultad de Ciencias de la Tierra y el Espacio, Universidad Autónoma de Sinaloa, Circuito Interior Oriente, Cd Universitaria, Culiacán, Sinaloa 80040, México
*Corresponding author. E-mail: jesus.rp@culiacan.tecnm.mx

## ABSTRACT

Urban storm drainage is essential for the large part of the population living in cities with torrential rains to protect public urban infrastructure, private property, and human lives from flooding. The most important design parameter for urban storm drainage is the flow discharge, which is normally calculated with the area, runoff coefficient, and rainfall intensity depending on basin delineation. This requires highly accurate topographic information on the urbanized terrain that digital elevation models sometimes do not meet due to the lack of resolution. This study proposes criteria for delineating urban basins considering urbanization without requiring the usual topographic surveys. The proposed urban basin delineation is based on a high-resolution digital elevation model obtained from an unmanned aerial vehicle (UAV) and field verification of flow directions. As a result, the delineation of two urban basins was obtained: an urban basin within an area that drains exclusively to a sinkhole and another basin that additionally drains out through other points of the divide. The latter basin does not comply with the traditional concept of a hydrological basin because it has more than one outlet. In addition, this basin has an area that is 38% of the total area draining into the sinkhole.

**Key words:** geospatial flow analysis, high accuracy DEM, UAV photogrammetry, urban basin delineation, urban hydrology, urban storm drainage

## HIGHLIGHTS

- Methodology to delineate urban basins based on UAV photogrammetry.
- Geospatial and surface flow direction analysis for urban basin delineation.
- More precise urban basin delineation that considers the layout of streets.
- Less expensive high-resolution topography to delineate urban basins.

## GRAPHICAL ABSTRACT

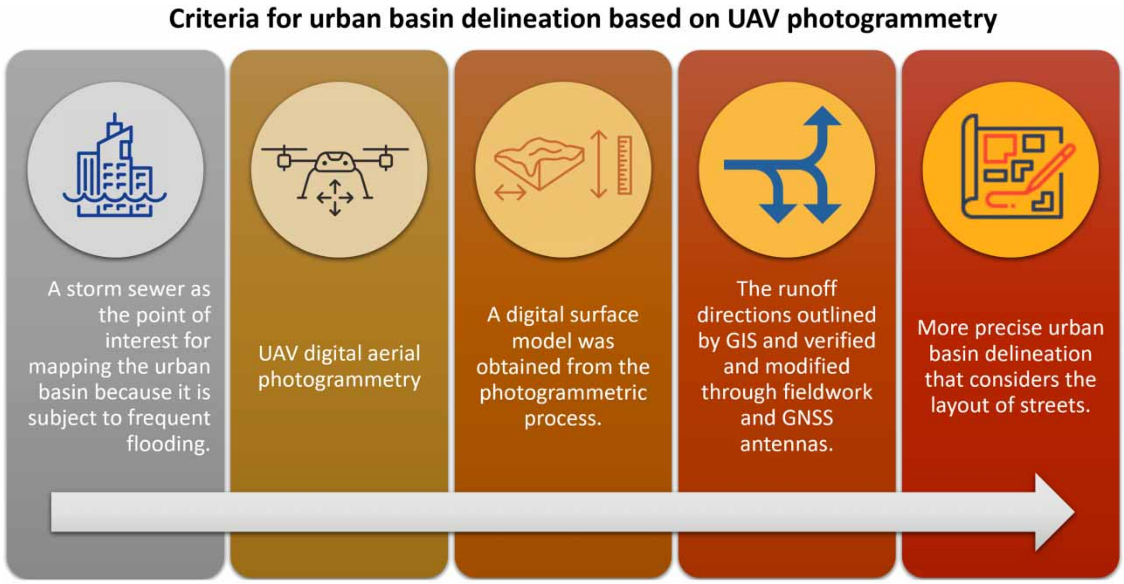


## 1. INTRODUCTION

Urban storm drainage is fundamental for the well-being of a large part of the population living in cities located in areas subject to torrential rains. This is because its function is to dislodge rainwater runoff to protect public urban infrastructure, personal property, and even human lives from flooding. Therefore, it is necessary to ensure its correct functioning and design. The main variable for the design of urban storm drainage is the design discharge, which normally depends on the area of the basin, the runoff coefficient, the time of concentration, and rainfall intensity. In turn, these variables depend on the delineation of the basin, which in the case of urban basins is not a trivial matter.

Population growth and urbanization lead to the modification of the natural hydrological conditions. For example, land-leveling alters overland runoff velocities; channelization tends to accelerate flow velocity and direction; the impervious surfaces (paving) increase the volume and velocity of surface runoff, while the development of storm sewer systems often imposes conditions of direction, outlets, times of concentration, and runoff catchment areas different from the original ones (Walesh 1989). These anthropogenic changes can direct water flows from one catchment area to another, modifying the hydrologic behavior of the natural basin and, consequently, its surface area.

Thus, the delineation of an urban basin is more complex than the delineation of a rural basin. This can usually be done efficiently from a digital terrain model using digital tools available. However, urban basins require procedures that consider the topography of the surface, which can be obtained through fieldwork or through digital surface models (DSMs) that include the urban layout of streets and buildings. Besides, the entire urban storm drainage system must be considered.

Conventional approaches used for rural basin delineation are unable to identify runoff transfers across modified topographic divides. Most of the studies conducted in urban basins are focused on managing urban stormwater runoff to mitigate flooding problems (de Almeida *et al.* 2018; Ariano & Oswald 2022; Ren *et al.* 2022). Few studies analyze the effect of changing natural water flow on the surface area of an urban basin and the changes in its delineation (Sokolovskaya *et al.* 2023). These studies require high-detail topographic information that may be scarce or non-existent due to the lack of resolution to map urban basins with the detail that hydrological studies require. In these cases, conventional topography must be carried out at the ground level, which represents a considerable consumption of time and economic resources.

Although the application of routine methods to delineate urban basins is widely recognized and used (Costa Rodrigues *et al.* 2022; Sharma *et al.* 2022), scarce studies describe the impact of urban development on the configuration of a natural drainage system. Parece & Campbell (2015) demonstrated a slight surface area variation in an urban basin when this basin was delineated using standard techniques for natural basins and 1-m resolution LiDAR. Rentería-Guevara *et al.* (2019)

demonstrated that an inappropriate delineation of an urban basin leads to serious inconsistencies in the calculation of surface water availability.

Procedures for delineating urban basins are scarce in the literature. Guidelines have been published in this regard (Abedin & Stephen 2019; Mihu-Pintilie *et al.* 2019; Gao *et al.* 2021), and some government authorities have established other guidelines for the delineation of catchment areas for urban drainage systems (USDA 1986; OECD 2012; DID 2012; CONAGUA 2019), but a procedure for delineating urban basins based on photogrammetry obtained using a unmanned aerial vehicle (UAV) has not been proposed and discussed. In this sense, this research proposes criteria for the delineation of an urban basin based on UAV photogrammetry, geospatial surface flow analysis, and fieldwork. As a case study, an urban basin delineation procedure was developed and applied in an area where the concentration of runoff causes frequent flooding in the city of Culiacan, Mexico. This paper proposes a methodology for the delineation of urban basins based on a high-resolution DSM and the directions of surface water flow over the roads. This procedure could be used in similar cases to improve the understanding of urban flooding where geomorphological information for basin delineation is scarce or non-existent.

## 2. MATERIALS AND METHODS

### 2.1. Study area

The study area is in the urban zone of the municipality of Culiacan, Sinaloa, Mexico, which is located between the latitude coordinates of 24°48′43.20″ and 24°48′21.56″, and longitudes of −107°22′22.78″ to −107°21′57.59″ (Figure 1). This geographic area is completely urbanized, mostly by housing development. The weather in the city during the rainy season is hot and mostly cloudy, while during the dry season, it is partly cloudy and hot. The air temperature generally varies from 12  to 36°C and rarely drops below 9°C or rises above 38 °C. According to the pluviometric stations closest to the study area, a maximum rainfall of 258 mm has been registered in the study area within 24 h (CONAGUA 2023). The wettest

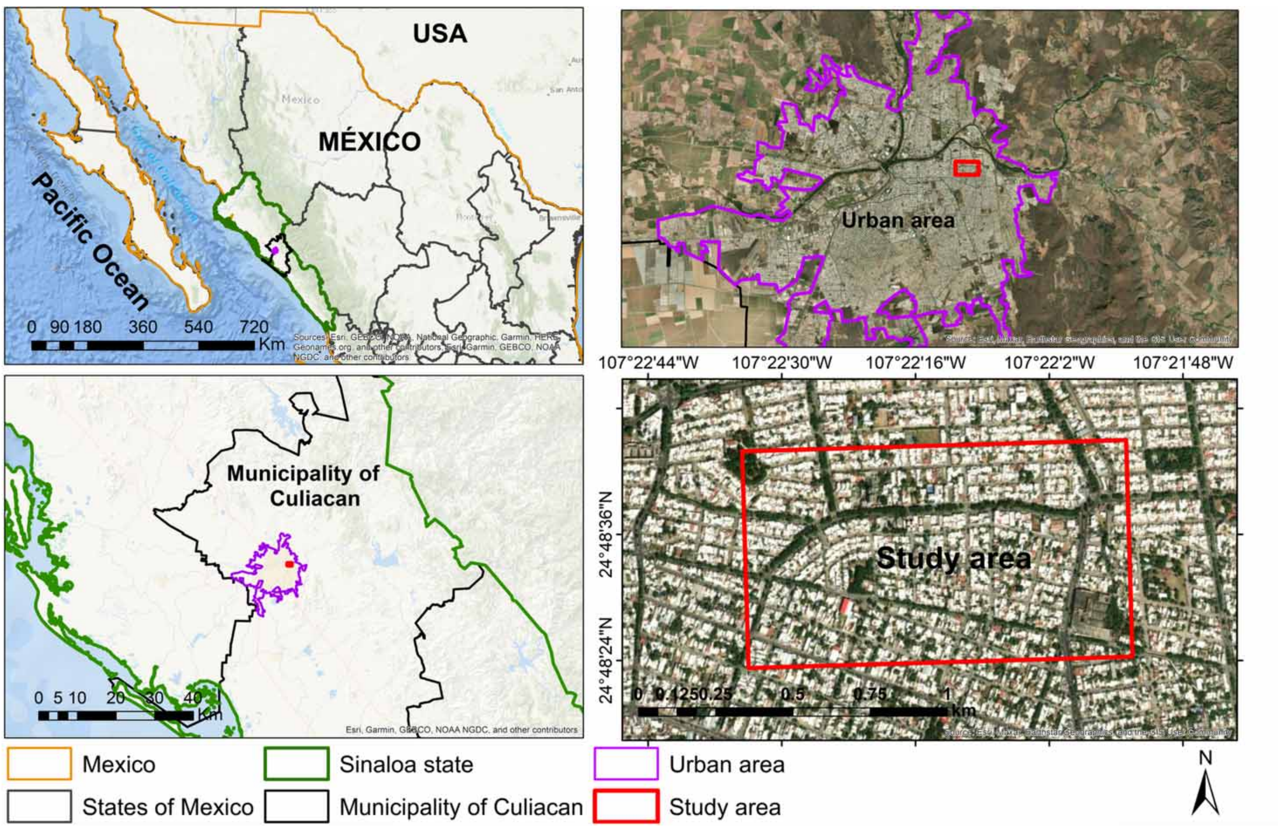


**Figure 1** | Study area location.

season lasts approximately 3 months, from June to September, and the driest season lasts almost 9 months, from September to June 24 (INEGI 2023a).

This area is an endorheic basin because surface flow accumulates in a sink not connected by surface channels or to other streams in the basin (WMO 2012). In our study, this sink is a storm sewer inlet that is the entrance to a subsurface drainage system.

The general surface water drainage pattern of this area follows the urban roads from south to north towards the Tamazula River, a tributary of the Culiacan River, which is the main runoff collector of the city. The discharge point (the inlet storm sewer) is at the intersection of a main street and a secondary street (Figure 3). The discharge captured by the sewer is conveyed through an underground pipe with a diameter of 90 cm along the main road until the flow is discharged into the river. The dimensions and layout of this underground drainage system were obtained by field inspection since there are no official plans.

## 2.2. Methodology

### 2.2.1. General outline of the methodology to delineate an urban basin by photogrammetry

The methodology followed in this study has advantages over traditional methodologies. The main advantage is the obtaining of the topography using photogrammetry, which facilitates a detailed study of important territorial extensions in a short time and at a low cost in areas of difficult access. A strength of the proposed methodology is the field verification of digitally defined flow directions and watershed divides. The general overview of this methodology is shown in Figure 2, while the description of each of the stages is described in the following sections.

### 2.2.2. Selection of a case of interest

The selection of the case study can be made according to academic or technical criteria. The objective is to delimit urban basins, which should be the basic units of geographic analysis of surface water flow patterns in cities. Their delineation can be used to support the understanding of the hydrological functioning of an urban area, the design of urban storm drainage works, or the review of the performance of existing works. The geographic extent of a case study is determined by the specific objective of the study and seeks to include the entire territory that drains stormwater runoff to the site or sites of interest. Such territory may include fully or partially urbanized areas of interest to different stakeholders.

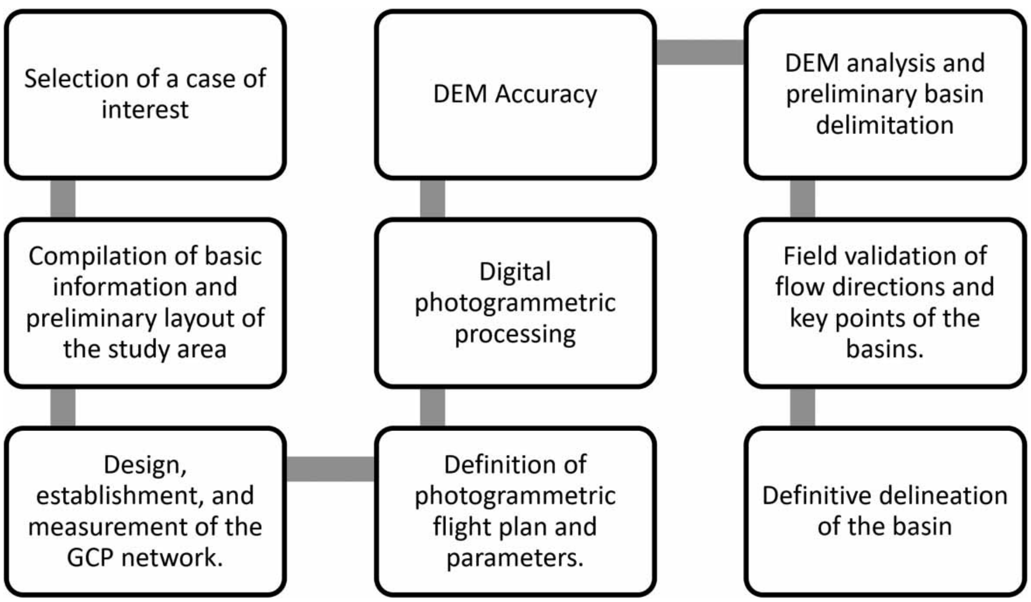


**Figure 2** | Flow chart of the proposed methodology to delineate an urban basin.

### 2.2.3. Compilation of basic information

To analyze our case study, hydrological information of the study area was requested to support the understanding of the storm drainage pattern; however, no previous basin delineations, topographic maps, digital elevation models (DEMs), or land use maps of the urban basin were found. Due to the scarcity of basic information, satellite images and a DEM with poor resolution (5 m), both freely available, were used to make a preliminary delineation of the urban basin under study.

### 2.2.4. Design, establishment, and measurement of the ground control point network

A network of ground control points (GCPs) was strategically designed and established. For this purpose, a pair of global navigation satellite system (GNSS) antennas, a base, and a rover (model HI Target v30 Plus multifrequency) were used.

A GNSS base point was established and measured in static mode for 3 h at 5 s intervals. This base point was processed and adjusted according to the National Active Geodetic Network (RGNA) of Mexico, using the station 'CULC' of the National Institute of Statistics and Geography (INEGI). Then, the GCP network established in the study area was measured using the real time kinematic technique to obtain the precise coordinates of the GCPs (Ekaso *et al.* 2020).

### 2.2.5. Definition of photogrammetric flight plan and parameters

An UAV model Phantom 4 PRO was used in this research to achieve greater accuracy and reliability in the DSM. The flight parameters were defined according to the expected accuracies and the objective of the research. A flight height of 100 m was set with a flight speed of 15 m/s, a camera angle of 90 degrees, and horizontal and transverse overlaps of 75 and 70% were used, respectively. Also, the polygon and the orientation of the flight lines were determined in DJI's GSP-PRO software and used to capture all the images of this research.

### 2.2.6. Digital photogrammetric processing

The images obtained by the photogrammetric flight were processed with the software Agisoft Metashape Professional. The workflow was based on Mora-Felix *et al.* (2020) and Elkhrachy (2021) and consisted of importing the images to this software and assigning the coordinate system WGS-84 UTM 13 N to each of the images. A preliminary external orientation was then applied to the images using 40,000 key points and 4,000 tie points per image. The GCP points measured in the field were added to improve the results. The GCPs were used to adjust the external orientation of the photographs considering the parameters of the camera model.

A dense point cloud was generated using a moderate filter to obtain more accurate results in the elevation coordinate (Mora-Felix *et al.* 2020). The DSM was created taking the dense point cloud as a reference, and the orthophotography was finally generated from the DSM (Elkhrachy 2021). The orthophotography and DSM were the main products of digital photogrammetry.

### 2.2.7. DSM accuracy

The accuracy of the DSM was determined by the root-mean-square error (RMSE) in planimetry and altimetry. According to Equations (1) and (2), the coordinates of the GCPs measured with the GNSS antennas are considered the 'true' observations and were compared to the coordinates obtained from the photogrammetric products (orthophotography and DSM) (Mora-Felix *et al.* 2020).

Equation (1) was used to measure the DSM accuracy in the two-dimensional plane:

$$\mathrm{RMSE}_{xy} = \sqrt{\frac{\sum_{i=1}^{n}\left[(X_o - X_{\mathrm{GCP}})^2 + (Y_o - Y_{\mathrm{GCP}})^2\right]}{n}} \tag{1}$$

where $X_0$, $Y_0$ is the coordinates obtained from the DSM for the $X$ and $Y$ axes, respectively; $X_{\mathrm{GCP}}$, $Y_{\mathrm{GCP}}$ is the coordinates taken in the field with GNSS antennas for the $X$ and $Y$ axes, respectively; and $n$ is the number of GCP points taken in the field.

Equation (2) was used to measure the DSM accuracy for elevation.

$$\mathrm{RMSE}_Z = \sqrt{\frac{\sum_{i=1}^{n}[(Z_o - Z_{\mathrm{GCP}})^2]}{n}} \tag{2}$$

where $Z_0$ is the coordinates obtained from the DSM for the $Z$ axis and $Z_{\mathrm{GCP}}$ is the coordinates taken in the field with GNSS antennas for the $Z$ axis.

#### 2.2.8. DSM analysis and preliminary basin delineation

Using QGIS software, the elevation profile of each road in the DSM was analyzed to identify the surface flow directions and the maximum elevations where the basin should be delineated. The lowest point in the DSM corresponds to the basin outlet point and the elevations from that point should be higher until they reach the maximum. Hence, the result of this analysis is two vector layers: one with arrows indicating the flow directions and the other with the basin delineated.

The flow directions were marked with arrows using the DSM and aerial orthophotography of the area in each of the most representative roads. This process was supported by the longitudinal terrain profile tool of QGIS, where the slopes of each of the roads were recognized. The process consisted of drawing a line (arrowhead) on the base map, starting from the maximum elevation, and following the direction of flow. The urban basin was obtained from the drawing of the maximum elevations identified in the DSM.

#### 2.2.9. Field validation of flow directions and key points of the basins

A field inspection was carried out to confirm or modify the digitally obtained flow directions and basin boundaries. This fieldwork was carried out to avoid data uncertainty due to the presence of obstacles, such as trees, buildings, or other types of infrastructure, that difficult the measure surface coordinates accurately. The maximum elevations and flow directions were validated in the study area by observing the slopes of the roads, the surface storm drainage works such as channels or ditches, and other details that supported the validation of the surface flow behavior, such as flooding marks on buildings, drainage works under construction, recently housing developments, and even interviews with neighbors in the area.

#### 2.2.10. Definitive delineation of the basin

Once the information was validated in the field, the procedure of drawing lines through the building terrain was not properly correct. This is because the terrain is normally leveled before construction, which commonly directs the surface flow to a point or edge of the terrain. As a general criterion, this methodology assumed that a terrain drains towards the streets in front of the edifications. This way, the urban basin delineation meets the contours of the building terrains and constitutes the definitive delineation. This delineation is hence characterized by straight lines forming angles, mainly of 90°, which differs from the sinuous lines that characterize the natural or rural basins.

## 3. RESULTS

### 3.1. Methodology to delineate an urban basin by photogrammetry

The main result of this research is a methodology to delineate urban basins. This methodology is original for urban basin delineation and has not been reported in the literature before since it combines the acquisition of orthophotos by UAV, their processing by geospatial techniques, and field validation. In addition, it adapts the contour of the basins to the urban layout respecting the roads as the physically operating channels of the surface drainage system of the urbanized land. Figure 2 shows the workflow of the proposed methodology.

### 3.2. Selection of a case of interest

The city of Culiacan is at the confluence of the Tamazula River and the Humaya River. This city is frequently affected by flooding on the banks of the rivers as well as in areas far from them. The first case is less frequent because these rivers are controlled by dams; however, non-riverine flooding is becoming more frequent due to the inadequacy of the storm drainage system. Government authorities recognize that frequent flooding occurs in populated residential areas of Culiacán and this phenomenon is therefore included in the Risk Atlas of Culiacan, Sinaloa (GeoEcoSphera 2020). According to this, an urban basin subject to flood risks in the city was selected. It is assumed that this happens mainly because the design flow of the storm sewer was not correctly calculated. Its calculation depends on the magnitude of the basin area, which in turn depends on the delineation of the basin. In addition, the flow pattern in the roads can influence the accumulation of rainwater because such flow can be directed or diverted to a point of interest depending on the urban layout.

By direct observation, the urban flooding was validated in a specific site of interest that was selected as a case study. This is the location of a grated storm-drain inlet in the vicinity of which, during the rainy season, flooding frequently occurs with significant depths and durations. This may mean insufficient collection capacity through the grated inlet, the storm sewer, or both. In any case, to solve the problem, it is advisable to determine the design flow that the storm drainage system should discharge at the site of interest. In the absence of direct measurement of the discharge, a fundamental variable for this purpose is the area of runoff contribution to the drainage point. This leads to the delineation of the basin whose outlet point is the location of the storm-drain inlet.

### 3.3. Compilation of basic information

Information on the study area was compiled, essentially the official hydrological delineation (INEGI 2023b) and the DEM (INEGI 2023c). No previous hydrological studies were located, neither urban layout maps nor the surface or subsurface storm drainage network. Using satellite images (Google 2023), a preliminary study area was drawn (Figure 3) to plan a field inspection and locate sites to install control points.

### 3.4. Design, establishment, and measurement of the GCP network

Through fieldwork, it was deduced that there is a subsurface storm drainage pipe located under the main avenue with an entrance under the grate and an exit on the left bank of the Tamazula River (Figure 3). In addition, the field survey was used to visualize the possible surface flow directions of the main roads. The surroundings of the grated inlet location were chosen as a preliminary study area to locate the GCPs (Figure 3).

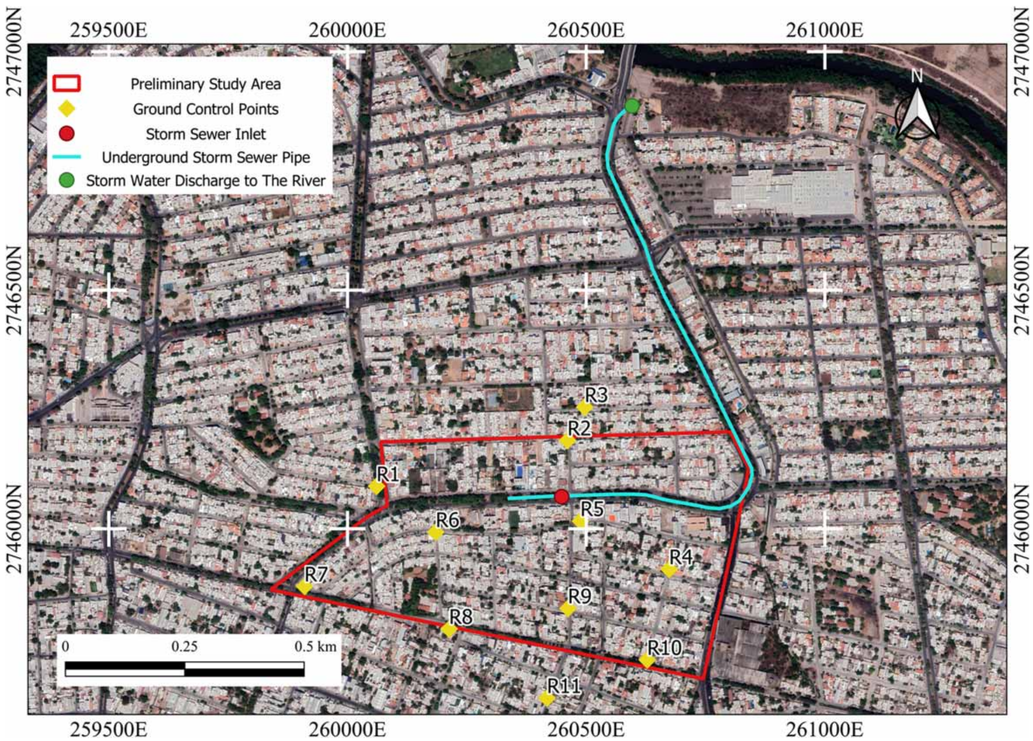


**Figure 3** | Location of the storm-sewer inlets, drainage pipes, and GCPs.

### 3.5. Definition of photogrammetric flight plan and digital photogrammetric processing

Two photogrammetric flights were carried out with a UAV, from which images of the study area were obtained. The images were processed in a digital photogrammetric system to obtain the main photogrammetric products: a DSM and an orthophotography with an accuracy of 2.7 cm/pixel (Figure 4).

### 3.6. DSM accuracy

The accuracy of the DSM was obtained from Equations (1) and (2). This accuracy was calculated using the photogrammetric products (orthophotography and the DSM). The planar coordinates on the *X* and *Y* axes were obtained from the planimetric model and the vertical *Z* coordinate was obtained from the DSM. A second set of data was obtained from GCPs, which were obtained with calibrated GNSS antennas. These points were considered true terrain measurements. Eleven control points were used, each of them with their respective elevations and the *X* and *Y* coordinates. Table 1 shows the values of the GCP and photogrammetric model coordinates.

The RMSE equations (Equations (1) and (2)) were applied with the coordinates obtained. The coordinates differences between DSM points are observed in Table 1. An RMSE of 0.0539 m was obtained in the horizontal two-dimensional plane and an RMSE of 0.04266 m in the vertical one-dimensional plane. The values obtained for RMSE are like those presented by Kršák *et al.* (2016), who demonstrated a satisfactory height difference of 0.0836 m for a DEM obtained using low-cost UAV photogrammetry in Jastrabá, Slovakia. Seifert *et al.* (2019) reported a planimetric accuracy range of 0.10–0.15 m. Thus, the photogrammetry obtained in our study is accurate and adequate to delimit an urban basin.

### 3.7. DSM analysis and preliminary basin delineation

Figure 5 shows an example of the elevation profile of a roadway in the DSM obtained in the study area. This profile was used to recognize the surface flow pattern. The process of identifying the flow directions of the tributaries of the urban basin was based on the evaluation of the longitudinal profile obtained from the DSM and subsequent fieldwork, as a method of verifying the resulting information.

The identification of the basin divides was fundamental to preliminarily establish the flow directions in each roadway (Figure 6), connecting the points or nodes by straight line segments as proposed by Gaspari *et al.* (2012).

The flow directions and key points of the basins were determined semi-automatically from the DSM of the study area (Sanhouse-García *et al.* 2021).

### 3.8. Field validation of flow directions and key points of the basins

The basin divides and flow directions were validated with the information from fieldwork. At this stage, the influence of the slope on the current and flow direction was evaluated. It was corroborated that, except for the storm-drain inlet that delimits the study basin, there are no other underground storm drainage structures. All the roads were inspected, visualizing in detail the direction of flow and the watercourses. Then, the flow directions of the tributaries and basin divides were edited on the previously generated base map in each case. In some cases, the GNSS receiver was used to verify the elevation of the terrain, which made it possible to accurately pinpoint some of the divides and to determine the definitive flow directions of the tributaries. It should be noted that more accurate results were obtained for the DSM in the preliminary phase.

### 3.9. Definitive delineation of the urban basin

The definitive delineation of the urban basin was carried out after verifying the flow directions and the points through which the basins pass. The result of this delineation is shown in Figure 7.

Figure 7 shows two delineations: one delineation closer to the drainage point (storm sewer inlet) whose area drains exclusively to the inlet (exclusive contribution area), and other areas farther away that drain partially to the inlet (area between urban basin lines and exclusive contribution area lines). This is noted by observing the flow directions which are directed towards the inlet, while others are away from it. This means that the urban basin delineated with the criteria proposed in this study has an area that drains exclusively to a single point, while the other delineation directs its runoff towards that point and out of the basin across several sites along its divide. The area of the basin that drains exclusively to the storm sewer inlet is 0.13 $km^2$, the area that drains partially is 0.08 $km^2$, while the total area of the urban basin is 0.21 $km^2$.

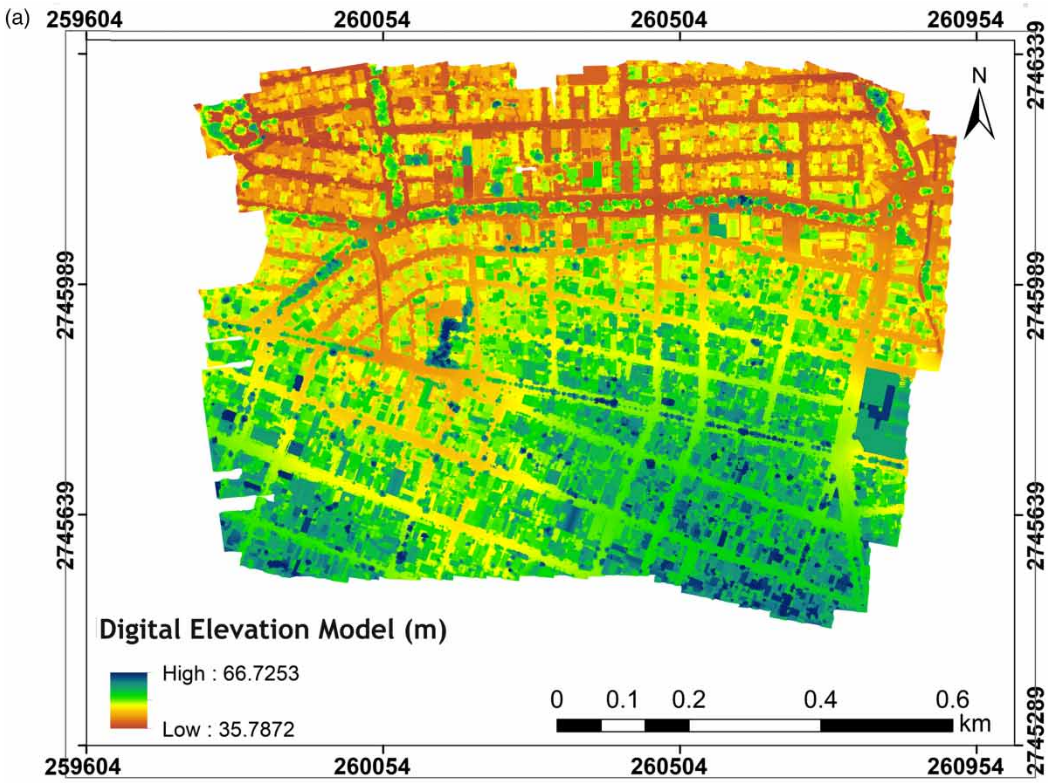


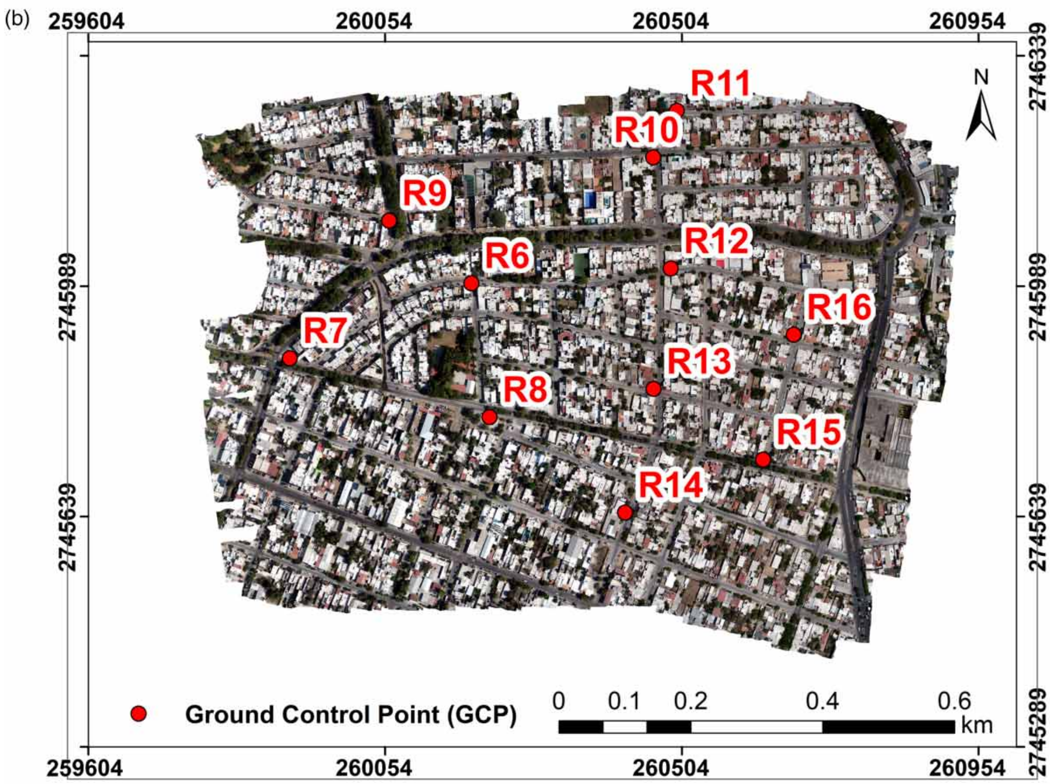


**Figure 4** | Digital surface model (a) and orthophotography (b) of the study area with the GCPs.

**Table 1** | Control points and DSM coordinates and their differences

| Name | GCP coordinates | | | DSM coordinates | | | Differences | | | | |
|---|---|---|---|---|---|---|---|---|---|---|---|
| | $X_{GCP}$ | $Y_{GCP}$ | $Z_{GCP}$ | $X_0$ | $Y_0$ | $Z_0$ | $X_{GCP}-X_0$ | $Y_{GCP}-Y_0$ | $Z_{GCP}-Z_0$ | $(X_{GCP}-X_0)^2+(Y_{GCP}-Y_0)^2$ | $(Z_{GCP}-Z_0)^2$ |
| R1 | 260,061.116 | 2,746,089.021 | 41.4384 | 260,061.125 | 2,746,089.180 | 41.39044 | −0.00956 | −0.15904 | 0.04796 | 0.02538 | 0.00230 |
| R2 | 260,461.598 | 2,746,185.261 | 42.4307 | 260,461.567 | 2,746,185.237 | 42.41827 | 0.03038 | 0.02359 | 0.01243 | 0.00147 | 0.00015 |
| R3 | 260,497.412 | 2,746,255.863 | 42.2888 | 260,497.399 | 2,746,255.851 | 42.28556 | 0.01287 | 0.01211 | 0.00324 | 0.00031 | 0.00001 |
| R4 | 260,674.631 | 2,745,915.847 | 47.5097 | 260,674.670 | 2,745,915.842 | 47.61637 | −0.03914 | 0.00517 | −0.10667 | 0.00155 | 0.01137 |
| R5 | 260,488.224 | 2,746,016.404 | 44.5997 | 260,488.225 | 2,746,016.397 | 44.56780 | −0.00093 | 0.00651 | 0.03190 | 0.00004 | 0.00101 |
| R6 | 260,185.911 | 2,745,993.768 | 44.3619 | 260,185.905 | 2,745,993.761 | 44.37762 | 0.00628 | 0.00714 | −0.01572 | 0.00009 | 0.00024 |
| R7 | 259,910.565 | 2,745,879.998 | 46.7243 | 259,910.586 | 2,745,880.035 | 46.72329 | −0.02099 | −0.03715 | 0.00101 | 0.00182 | 0.00000 |
| R8 | 260,213.489 | 2,745,790.568 | 47.3464 | 260,213.503 | 2,745,790.581 | 47.38697 | −0.01401 | −0.01266 | −0.04057 | 0.00035 | 0.00164 |
| R9 | 260,462.160 | 2,745,833.448 | 49.1001 | 260,462.171 | 2,745,833.433 | 49.12516 | −0.01092 | 0.01543 | −0.02506 | 0.00035 | 0.00062 |
| R10 | 260,628.277 | 2,745,725.864 | 51.1955 | 260628.263 | 2,745,725.867 | 51.22867 | 0.01321 | −0.00339 | −0.03317 | 0.00018 | 0.00110 |
| R11 | 260,418.904 | 2,745,645.384 | 52.0369 | 260,418.900 | 2,745,645.405 | 51.99763 | 0.00477 | −0.02089 | 0.03927 | 0.00045 | 0.00154 |
| | | | | | | | | | $\sum =$ | 0.03205 | 0.02002 |
| | | | | | | | | | **$\text{RMSE}_{XY}=$** | **0.054** | |
| | | | | | | | | | | **$\text{RMSE}_{Z}=$** | **0.043** |

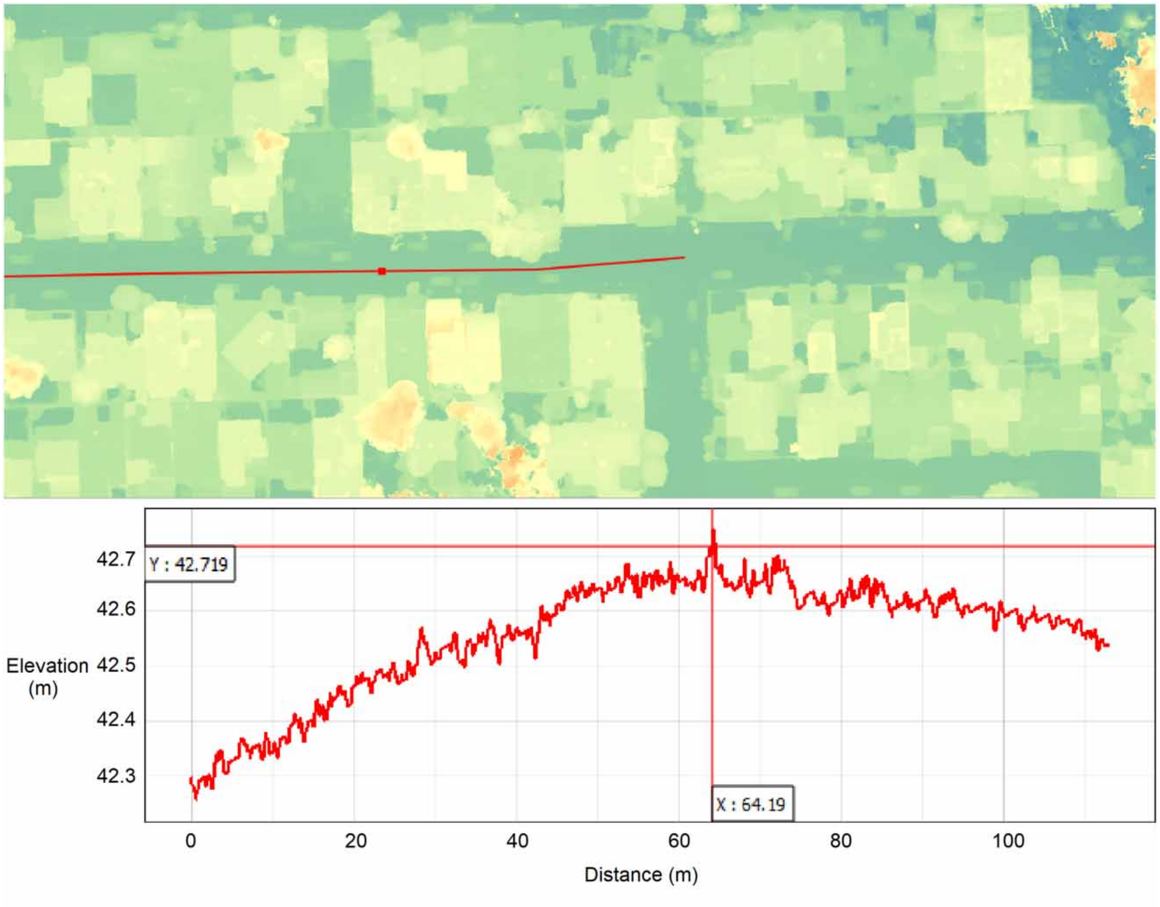


**Figure 5** | Elevation profile of roadway defining a point in a basin divide.

### 3.10. Other basin delineations in the study area

For comparison purposes, the official hydrological delineation of INEGI (2023b) for the study area is presented (Figure 8). This is in the official Rio Tamazula sub-basin, code RH10Cb, which has a territorial extension of 1,955.0 km$^2$. In addition, the INEGI (2023c) DEM with a resolution of 5 m per pixel was used to generate sub-basins using the automatic option of QGIS. According to this procedure, four sub-basins were generated in the study area, which are indicated with the numbers 1–4 in Figure 8. These sub-basins have areas of 4.25, 2.23, 14.48, and 0.30 km$^2$, respectively.

## 4. DISCUSSION

Typically, a DEM is used to identify basin divides (Jancewicz *et al.* 2022). By using a DEM, points of flow convergence (stream network) and divergence (basin divide) can be identified. A general process of basin delineation in GIS is proposed by Abedin & Stephen (2019). For this process, the resolution of DEM is a determining factor for the delineation of a basin (Ariza-Villaverde *et al.* 2015; Nazari-Sharabian *et al.* 2020). High spatial resolution DEMs can be obtained from airborne LiDAR technology. Mihu-Pintilie *et al.* (2019) used the raw ground point elevation data from the National Administration Romanian Waters (NARW) at a spatial density between 0.5 and 3 m to delineate the urban basin in Bacau City in Northeast Romania. However, the use of LiDAR technology is limited for urban basin delineation since LiDAR data coverage worldwide is minimal due to its high cost (Muhadi *et al.* 2020).

Hence, UAVs represent an alternative to satellites or airplanes since they provide high spatial terrain details essential for hydrological delineation and modeling (Avila-Aceves *et al.* 2023). Ouédraogo *et al.* (2014) assessed the impact of intensive farming activities on small agricultural basins. They used terrestrial laser scanning and unmanned aerial system photogrammetry to generate accurate and high-resolution DEMs in a small basin area (12 ha). They reported that the agricultural basin

**Figure 6** | Definition of the preliminary flow directions of the roads by DSM analysis.

topography varied depending on the crops that were cultivated. The presence of crops, crop residues, furrows, and ridges modified the direction of water flow and the runoff and sediment transport. Mansoori *et al.* (2019) described the drainage patterns of the Hatta catchment in a mountainous region of the United Arab Emirates. Hydrological features, such as flow direction, flow accumulation, stream definition, stream segmentation, and watershed delineation, were obtained using a 23-cm ground resolution DEM obtained from photogrammetric techniques with high-resolution images captured via fixed-wing drones. No risk of flash floods was identified in the study area since the stream flows are controlled by a dam.

In our study, the high spatial terrain details obtained from a photogrammetric survey and processing were used to analyze an urban basin where frequent flooding occurs. The methodology consisted of acquiring stereo images using a UAV. Then, these images were processed to generate a high-resolution DEM. The maximum elevations of the zone were identified through geospatial analysis, and the runoff flow directions were outlined considering the topography modifications because of urban developments. As a result, the delineation of an urban basin that drains only to a sewer is provided with accurate planimetric and altimetric results.

Scarce studies are given in the literature to delineate urban basins considering the surface and underground drainage network. Walesh (1989) presented a comparison between the results of delineating 12 urban basins based on topographic maps and the delineation obtained of the same basins verified in the field. The study showed catchment area differences between 13 and 490%, which were attributed to terrain leveling, urban drainage, and map resolution. Kayembe & Mitchell (2018) found differences between 5 and 8% comparing a topographically delineated basin and one delineated using a semi-automated approach incorporating conventional drainage networks. In our research, an urban basin was delineated using innovative techniques involving digital aerial photogrammetry with UAV, geospatial analysis techniques, and surface flow direction analysis. According to the results obtained, a catchment area difference of 23.8% was found for the automated delineation.

The procedure described in our study revealed that the area of contribution to the sewer does not coincide with the area of a hydrological basin delineated based on the identification of high points on the streets. This is because the basin area

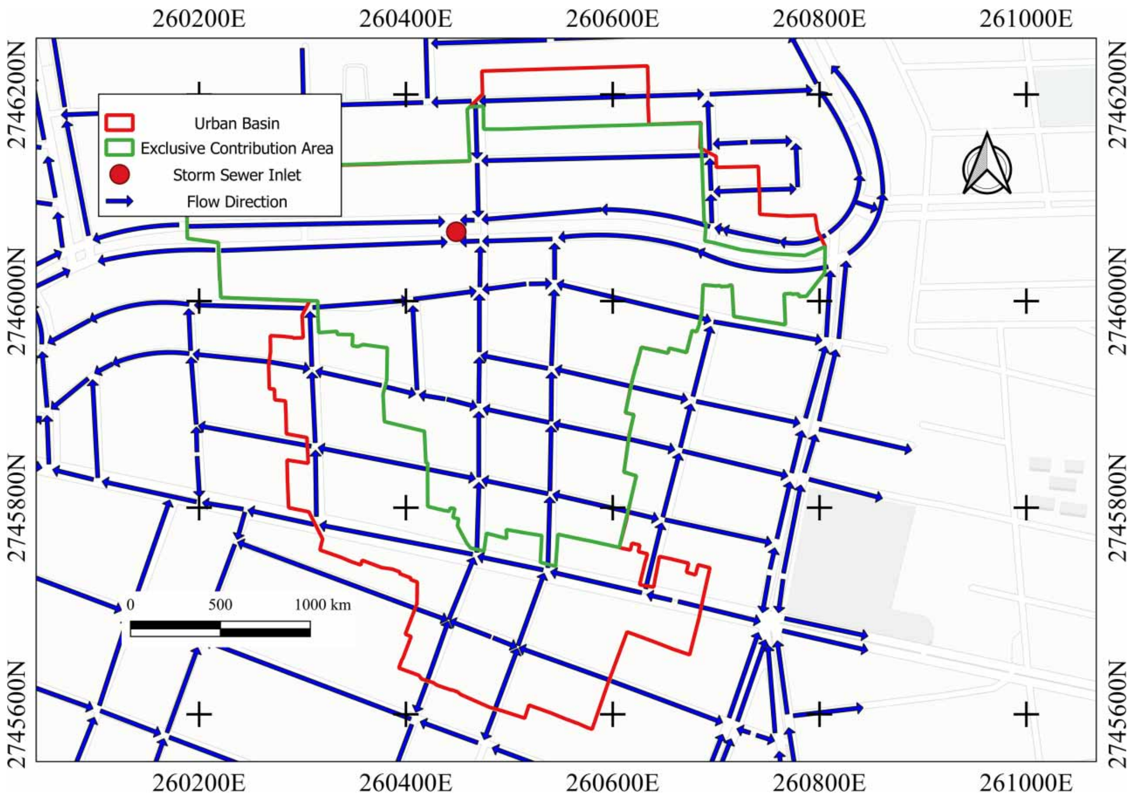


**Figure 7** | Delineation of the urban basin and the sewer contribution area.

contains a part that drains only to the storm sewer inlet and another part that drains to the storm sewer inlet and out of the basin across its divide. Thus, the traditional procedures for estimating runoff in urban basins based on the formal concept of the basin should be applied with caution. As a first approximation, in this study, it was estimated that the runoff area draining only to the storm sewer inlet is 62.0% of the runoff captured by the entire basin. This estimation is based on the ratio of the areas.

Radwan *et al.* (2020) and Natarajan & Radhakrishnan (2019) delineated urban basins using techniques normally applied to delineate natural basins. This approach has the disadvantage of not considering the transfer of flow through topographic basins due to urban storm drainage works, the creation of sinkholes, and the modification of the natural topography. The urban basin under study has a drainage point with a sinkhole but does not present the other forms of flow transfer; nevertheless, the criteria proposed in our investigation consider these forms of transfer in the delineation of an urban basin.

From a 2 $m^2$ DEM obtained with LIDAR technology, Parece & Campbell (2015) delineated a small urban basin using standard techniques for natural basins supported by digital processing of information on storm drainage works that affected the flow pattern. In this way, to delineate the urban basin, they connected and disconnected areas of surface flow input whose outflows were removed through subsurface drainage. In our study, this was not necessary because no partial areas connected or disconnected with the basin under study were detected. Furthermore, in contrast to the methodology of Parece & Campbell (2015), the methodology proposed in the present research includes field validation of the basins.

We admit that the application of our procedure presented some drawbacks. One of them was the lack of information on the layout of the subsurface storm drainage network. This information could generate a more accurate model with a complete hydraulic functioning of the area. This situation limited the analysis of the surface runoff on roads, open areas, and building roofs. It was considered that the runoff drained towards the front of the buildings, although it could be analyzed in greater detail using the resolution of the model (2.7 cm). However, this would imply knowing the route of the water through the drains inside the buildings, which would be complicated, especially in the interior storm sewers.

The basin mapping using the INEGI's DEM has the advantage that it is of free use. However, its resolution is low for a detailed analysis such as the one presented in this manuscript. The official INEGI basin in Figure 8 is too large to perform

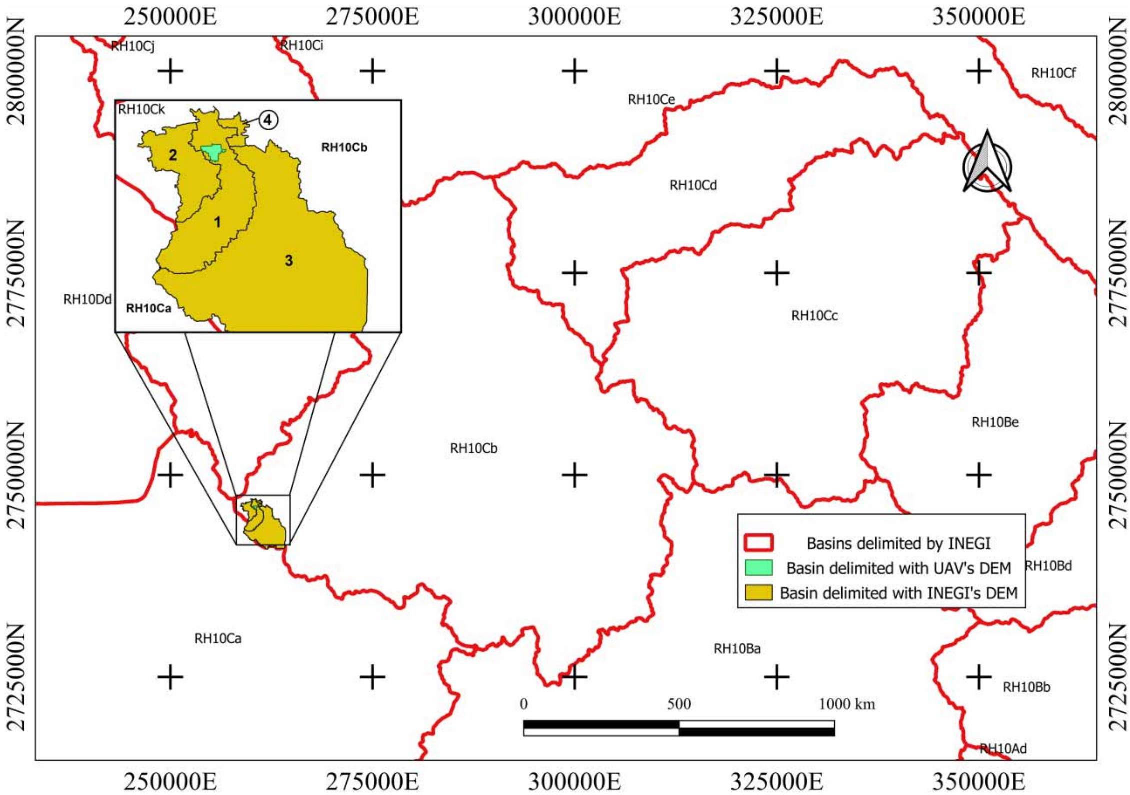


**Figure 8** | Official INEGI delineation, basins mapped with the INEGI DEM, and urban basin delimited by UAV photogrammetry in the study area.

the detailed analysis required for a problem such as the one addressed in this research. The estimation of the design flow for a storm drainage structure requires a greater resolution model. The INEGI's DEM is 5 m per pixel, which makes it difficult to accurately analyze the flow in roads with minor slopes, which sometimes have only a few centimeters of elevation.

## 5. CONCLUSIONS

The delineation of an urban basin is more complex than the delineation of a natural basin. The automatic GIS procedures do not consider the influence of urbanization on the surface flow pattern. These automated procedures represent the terrain without urban infrastructure. Urban layout, urban drainage works, interaction with underground drainage, and modification of natural terrain slopes make it difficult to reliably delineate urban basin boundaries. Therefore, it is not convenient to grant that urban hydrology or urban storm drainage studies involve a correct delineation of basins because of the application of automated or systematized procedures.

This study demonstrated that the area of an urban basin differs from the area of contribution to a surface outflow. In this sense, it is desirable to apply the criteria presented here for delineating urban basins to other urban study areas. In addition, it would be desirable to apply the criteria of this research to urban basins with flow transfers through underground storm drainage works, as well as detention and retention ponds and other storm drainage works. These aspects would support a better understanding of flow patterns and would strengthen the criteria for delineating urban basins presented in this work.

The methodology proposed in this study offers advantages over other approaches, including a lower cost and time requirement for obtaining topography. This is especially beneficial compared to costly ground-level surveys, which are time-consuming and labor-intensive. This methodology provides a high-resolution DSM that most of the time is not freely available. Many times, the DEMs available for free lack resolution to map an urban basin with the necessary detail to analyze the flow could be the reason for non-satisfactory storm drainage projects. Our methodology also includes field verification of the surface flow directions and, consequently, of the main points of the watershed divides. This allows a better representation of the surface flow pattern.

Similar conditions in terms of vulnerability to flooding and scarcity of information could be present in other urban basins such as the studied in the urban area of Culiacan. This suggests the need to develop procedures for mapping urban basins such as the one presented in this research. Our methodology can be applied in cities where photogrammetric flights are feasible and there is a need to map urban basins or revise existing basin delimitations.

The application of our procedure presented some limitations, such as the lack of information on the layout of the subsurface storm drainage network. With this information, a more accurate model with a complete hydraulic functioning of the area could be provided. In addition, the runoff in the study area was calculated as part of the total area of the basin. Therefore, a more detailed calculation is required for a better estimation of the design flow. Future work is planned to model the surface flow through the streets.

## ACKNOWLEDGEMENTS

The authors thank the Autonomous University of Sinaloa for providing the infrastructure to carry out this work. We also thank CONAHCYT for the economic support provided to the authors through SNII funds.

## AUTHOR CONTRIBUTIONS

S.A.R.G. conceptualized the study, performed methodology, investigated the work, wrote the original draft preparation, and reviewed and edited the manuscript. J.G.R.P. conceptualized the work, did formal analysis, wrote the original draft preparation, and reviewed and edited the manuscript. A.R.B. studied software, did formal analysis, visualized the work, and found resources. S.A.M.A. performed methodology, found resources, carried out data curation, supervised the work, and wrote, reviewed and edited the manuscript. A.J.S.G. performed methodology, studied software, visualized and validated the work. F.G.P. conceptualized, validated, and supervised the work, and administered the project.

## FUNDING

This work was supported by the Autonomous University of Sinaloa (PROFAPI PRO_A1_033).

## DATA AVAILABILITY STATEMENT

All relevant data are included in the paper or its Supplementary Information.

## CONFLICT OF INTEREST

The authors declare there is no conflict.

## REFERENCES


Abedin, S. J. H. & Stephen, H. 2019 GIS framework for spatiotemporal mapping of urban flooding. *Geosciences* **9**, 77. doi:10.3390/geosciences9020077.

Ariano, S. S. & Oswald, C. J. 2022 Broad scale assessment of key drivers of streamflow generation in urban and urbanizing rivers. *Hydrological Processes* **36** (4), e14579. doi:10.1002/HYP.14579.

Ariza-Villaverde, A. B., Jiménez-Hornero, F. J. & Gutiérrez de Ravé, E. 2015 Influence of DEM resolution on drainage network extraction: A multifractal analysis. *Geomorphology* **241**, 243–254. doi:10.1016/j.geomorph.2015.03.040.

Avila-Aceves, E., Plata-Rocha, W., Monjardin-Armenta, S. A. & Rangel-Peraza, J. G. 2023 Geospatial modelling of floods: A literature review. *Stochastic Environmental Research and Risk Assessment*. doi:10.1007/s00477-023-02505-1.

CONAGUA. 2019 *Drinking Water, Sewerage and Sanitation Manual*. CONAGUA, Mexico City (in Spanish).

CONAGUA. 2023 *Climatological Statistical Information*. Available from: https://smn.conagua.gob.mx/es/climatologia/informacion-climatologica/informacion-estadistica-climatologica (accessed 27 June 2023).

Costa Rodrigues, M. V., Guimarães, D. V., Borelli Galvão, R., Patrick, E. & Fernandes, F. 2022 Urban watershed management prioritization using the rapid impact assessment matrix (RIAM-UWMAP), GIS and field survey. *Environmental Impact Assessment Review* **94**, 106759. doi:10.1016/j.eiar.2022.106759.

de Almeida, G. A. M., Bates, P. & Ozdemir, H. 2018 Modelling urban floods at submetre resolution: Challenges or opportunities for flood risk management? *Journal of Flood Risk Management* **11**, S855–S865. doi:10.1111/JFR3.12276.

DID. 2012 *Urban Stormwater Management Manual*. Department of Irrigation and Drainage Malaysia, Kuala Lumpur, Malaysia.

Ekaso, D., Nex, F. & Kerle, N. 2020 Accuracy assessment of real-time kinematics (RTK) measurements on unmanned aerial vehicles (UAV) for direct geo-referencing. *Geo-spatial Information Science* **23** (2), 165–181. doi:10.1080/10095020.2019.1710437.

Elkhrachy, I. 2021 Accuracy assessment of low-cost unmanned aerial vehicle (UAV) photogrammetry. *Alexandria Engineering Journal* **60** (6), 5579–5590. doi:10.1016/j.aej.2021.04.011.

Gao, P., Gao, W. & Ke, N. 2021 Assessing the impact of flood inundation dynamics on an urban environment. *Natural Hazards* **109**, 1047–1072. doi:10.1007/s11069-021-04868-6.

Gaspari, F. J., Rodríguez Vagaría, A. M., Senisterra, G. E., Denegri, G. A., Besteiro, S. & Delgado, M. I. 2012 Caracterización morfométrica de la cuenca alta del río Sauce Grande, Buenos Aires, Argentina. *AUGMDOMUS* **4** (4), 143–158.

GeoEcoSphera 2020 *The Risk Atlas of Culiacan, Sinaloa*. Protección Civil, Culiacán (In Spanish).

Google 2023 Google Earth. Available from: https://www.google.com/intl/es-419/earth/ (accessed 27 June 2023).

INEGI 2023a Climatology of Mexico. Available from: https://www.inegi.org.mx/temas/climatologia/ (accessed 27 June 2023).

INEGI 2023b Hydrology Maps of Mexico. Available from: https://www.inegi.org.mx/temas/hidrologia/ (accessed 27 June 2023).

INEGI 2023c Elevation Maps of Mexico. Available from: https://www.inegi.org.mx/temas/relieve/continental/ (accessed 27 June 2023).

Jancewicz, K., Różycka, M., Szymanowski, M., Kryza, M. & Migoń, P. 2022 Topographic characteristics of drainage divides at the mountain-range scale – A review of DTM-based analytical tools. *ISPRS International Journal of Geo-Information* **11**, 116. doi:10.3390/ijgi11020116.

Kayembe, A. & Mitchell, C. P. J. 2018 Determination of subcatchment and watershed boundaries in a complex and highly urbanized landscape. *Hydrological Processes* **32** (18), 2845–2855. doi:10.1002/HYP.13229.

Kršák, B., Blišťan, P., Pauliková, A., Puškárová, P., Kovanič, Ľ., Palková, J. & Zelizňaková, V. 2016 Use of low-cost UAV photogrammetry to analyze the accuracy of a digital elevation model in a case study. *Measurement* **91**, 276–287. doi:10.1016/j.measurement.2016.05.028.

Mansoori, S. A., Al-Ruzouq, R., Dogom, D. A., Al Shamsi, M., Mazzm, A. A. & Aburaed, N. 2019 Photogrammetric Techniques and UAV for Drainage Pattern and Overflow Assessment in Mountainous Terrains – Hatta/UAE. In: *IGARSS 2019 - 2019 IEEE International Geoscience and Remote Sensing Symposium*, July 28–August 2, Yokohama, Japan. doi:10.1109/igarss.2019.8898151.

Mihu-Pintilie, A., Cîmpianu, C. I., Stoleriu, C. C., Pérez, M. N. & Paveluc, L. E. 2019 Using high-density LiDAR data and 2D streamflow hydraulic modeling to improve urban flood hazard maps: A HEC-RAS multi-scenario approach. *Water* **11**, 1832. doi:10.3390/w11091832.

Mora-Felix, Z. D., Sanhouse-Garcia, A. J., Bustos-Terrones, Y. A., Loaiza, J. G., Monjardin-Armenta, S. A. & Rangel-Peraza, J. G. 2020 Effect of photogrammetric RPAS flight parameters on plani-altimetric accuracy of DTM. *Open Geosciences* **12** (1), 1017–1035. doi:10.1515/GEO-2020-0189.

Muhadi, N. A., Abdullah, A. F., Bejo, S. K., Mahadi, M. R. & Mijic, A. 2020 The use of LiDAR derived DEM in flood applications: A review. *Remote Sensing* **12** (14), 2308. doi:10.3390/rs12142308.

Natarajan, S. & Radhakrishnan, N. 2019 Simulation of extreme event-based rainfall–runoff process of an urban catchment area using HEC-HMS. *Modeling Earth Systems and Environment* **5**, 1867–1881. doi:10.1007/s40808-019-00644-5.

Nazari-Sharabian, M., Taheriyoun, M. & Karakouzian, M. 2020 Sensitivity analysis of the DEM resolution and effective parameters of runoff yield in the SWAT model: A case study. *Journal of Water Supply: Research and Technology-Aqua* **69** (1), 39–54. doi:10.2166/aqua.2019.044.

OECD. 2012 *Redefining 'Urban": A New Way to Measure Metropolitan Areas*. OECD Publishing, Paris, France. doi:10.1787/9789264174108-en.

Ouédraogo, M. M., Degré, A., Debouche, C. & Lisein, J. 2014 The evaluation of unmanned aerial system-based photogrammetry and terrestrial laser scanning to generate DEMs of agricultural watersheds. *Geomorphology* **214**, 339–355. doi:10.1016/j.geomorph.2014.02.01.

Parece, T. E. & Campbell, J. B. 2015 Identifying urban watershed boundaries and area, Fairfax County, Virginia. *Photogrammetric Engineering and Remote Sensing* **81** (5), 365–372. doi:10.14358/PERS.81.5.365.

Radwan, F., Alazba, A. A. & Mossad, A. 2020 Analyzing urban watersheds morphometric in arid and semiarid regions using the complementarity of RST and GIS. *Arabian Journal of Geosciences* **13**, 1237. doi:10.1007/s12517-020-06161-5.

Ren, H., Liu, S., Li, M., Zhang, H., Wang, H., Hao, X. & Cui, J. 2022 Topological analysis and application of urban drainage network. *Water* **14** (22), 3732. doi:10.3390/W14223732.

Rentería-Guevara, S. A., Rangel-Peraza, J. G., Rodríguez-Mata, A. E., Amábilis-Sosa, L. E., Sanhouse-García, A. J. & Uriarte-Aceves, P. M. 2019 Effect of agricultural and urban infrastructure on river basin delineation and surface water availability: Case of the Culiacan River Basin. *Hydrology* **6** (3), 58. doi:10.3390/HYDROLOGY6030058.

Sanhouse-García, A. J., Rangel-Peraza, J. G., Rentería-Guevara, S. A., Bustos-Terrones, Y. A., Mora-Félix, Z. D., Plata-Rocha, W. & Monjardin-Armenta, S. A. 2021 Flood-prone area delineation in urban subbasins based on stream ordering: Culiacan urban basin as a study case. *Sustainability* **13**, 13513. doi:10.3390/su132413513.

Seifert, E., Seifert, S., Vogt, H., Drew, D., van Aardt, J., Kunneke, A. & Seifert, T. 2019 Influence of drone altitude, image overlap, and optical sensor resolution on multi-view reconstruction of forest images. *Remote Sensing* **11**, 1252. doi:10.3390/rs11101252.

Sharma, V. K., Azad, R. K., Chowdary, V. M., Jha, C. S., 2022 Delineation of frequently flooded areas using remote sensing: A case study in part of Indo-Gangetic Basin. In: *Geospatial Technologies for Land and Water Resources Management* (Pandey, A., Chowdary, V. M., Behera, M. D. & Singh, V. P., eds). Water Science and Technology Library, Springer, Cham, p. 103. doi:10.1007/978-3-030-90479-1_27.

Sokolovskaya, N., Vaughn, C., Jahangiri, H., Smith, V., Wadzuk, B., Ebrahimian, A. & Nyquist, J. 2023 Variability of urban drainage area delineation and runoff calculation with topographic resolution and rainfall volume. *Water Science and Technology* **87** (6), 1349–1366. doi:10.2166/WST.2023.072.

USDA. 1986 *Urban Hydrology for Small Watersheds. Technical Release No. 55*, 2nd edn. Soil Conservation Service, Washington, DC, USA.

Walesh, S. G. 1989 *Urban Surface Water Management*, 1st edn. Wiley, Valparaiso, IN, USA.

WMO. 2012 *International Glossary of Hydrology*. Available from: http://unesdoc.unesco.org/images/0022/002218/221862M.pdf (accessed 27 June 2023).

First received 29 June 2023; accepted in revised form 14 November 2023. Available online 22 November 2023